

COMPARISON OF IMAGES WITH DIRECT AND INDIRECT ILLUMINATION: LUNAR PERMANENTLY SHADOWED REGION ANALOG IMAGES A. C. Martin¹, B. W. Denevi¹, E. J. Speyerer², T. J. Thompson², H. M. Brown², A. K. Boyd², M. S. Robinson². ¹Johns Hopkins University Applied Physics Laboratory, Laurel, MD, 20723, USA. ²School of Earth and Space Exploration, Arizona State University, Tempe, AZ, 85281, USA. (anna.martin@jhuapl.edu)

Introduction: Lighting and viewing angles affect the appearance of surface features, and thus their geologic interpretation. While these photometric effects are well understood under direct illumination conditions, interpreting the geology of lunar permanently shadowed regions (PSRs) is complicated by the fact that PSRs receive no direct illumination, but only diffuse secondary illumination reflected at various angles from nearby sunlit surfaces [1], (termed “indirect illumination”).

Using Lunar Reconnaissance Orbiter Camera (LROC) Narrow Angle Camera (NAC) [2] images, we document how morphology and albedo features appear under direct and indirect illumination conditions to see how illumination affects appearance. The goal of this work is to provide an improved basis for the interpretation of LROC NAC observations of PSRs and to aid in the interpretation of images that will be acquired by future PSR imaging experiments such as ShadowCam onboard the Korean Pathfinder Lunar Orbiter (KPLO) [3].

Methodology: PSR Analog Imaging Campaign: We collected a set of 41 LROC NAC images of mid-latitude craters at large incidence angles ($>69^\circ$) to simulate the illumination conditions present within PSRs. Under these conditions, large shadows were cast across the crater and only light scattered from the upper wall illuminated the shadowed interior; image exposure times were set $>20\times$ longer than typical to acquire adequate signal within the shadowed regions. By comparing these indirect illumination images to other images of the same surface under direct lighting, we can better interpret the features visible within

indirect lighting NAC observations.

Surface Features: To assess the visibility of various surface features under indirect lighting, we mapped common morphologic features (blocky walls, tectonic expressions, and floor fractures). To assist with comparisons between the direct and indirect illumination images and other relevant datasets we considered multiple data sets for each region: the indirect illumination image, multiple mosaics created from images acquired under direct lighting with unique incidence angles (as close to 0° , 30° , 60° as possible), LRO Miniature Radio Frequency (Mini-RF) S-band map, the corresponding Mini-RF circular polarization ratio (CPR) map [4], along with a hillshade map from the SLDEM [5]. With these data sets, features within the crater could be compared across a wide range of illumination conditions and the influence of surface properties such as roughness and slope could be assessed.

Rayed craters and mass wasting features were mapped in QGIS. Features were first identified and mapped in images with indirect illumination then mapped again using multiple images with direct illumination images (Fig. 1). Mass wasting streaks (Fig. 2) were categorized depending on their reflectance relative to their surroundings.

Illumination Modeling: A model that simulates secondary illumination at each pixel inside each crater [6] documented the varied illumination received at each pixel. For each image the local primary illumination was determined from footprint and time of acquisition using NAIF SPICE and a NAC digital terrain model. Viewfactors (visibility of and relative

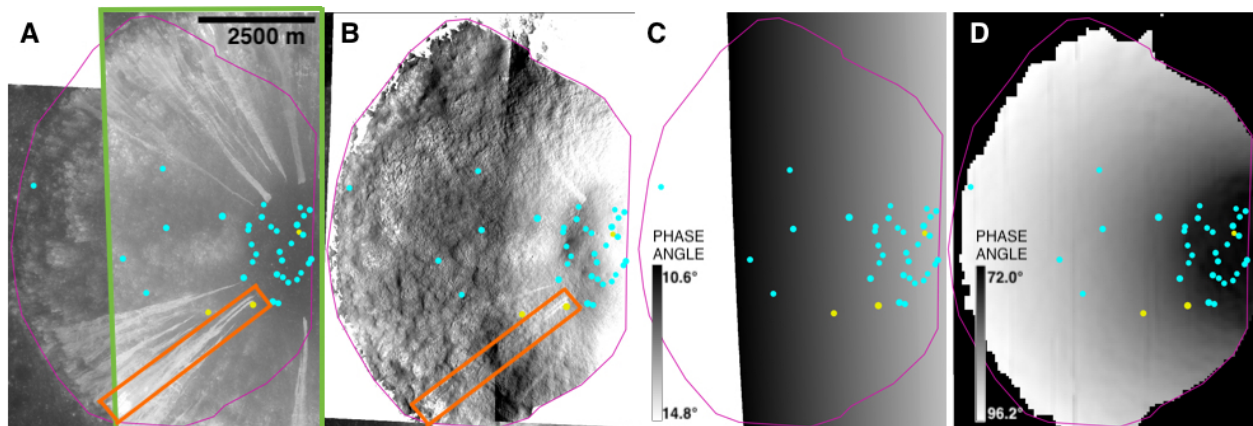


Figure 1: A portion of Lalande A crater (-6.6° lat, 350.1° lon, 12.25km diameter): A) direct illumination image mosaic, incidence angle is $\sim 13^\circ$; B) indirect (PSR-like) illumination stretched to highlight shadowed region (purple outline), incidence angle is $\sim 69^\circ$; C) map of phase angles of image pair M1195488314 (green box in panel A); D) map of the mean phase angles modeled for indirect illumination conditions in panel B. Phase maps are both stretched from 0.5–99.5% of their mean value. Small craters with high-reflectance ejecta are indicated in blue (identified only in direct illumination) and yellow (also observed in indirect illumination). Orange box corresponds to region shown in Fig. 2.

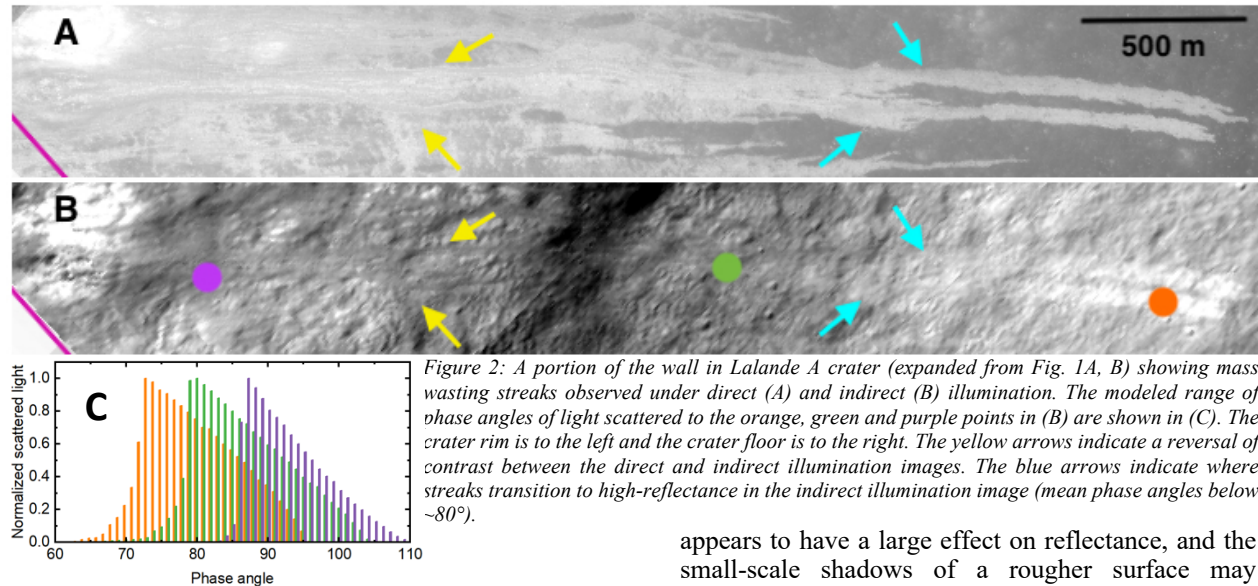


Figure 2: A portion of the wall in Lalande A crater (expanded from Fig. 1A, B) showing mass wasting streaks observed under direct (A) and indirect (B) illumination. The modeled range of phase angles of light scattered to the orange, green and purple points in (B) are shown in (C). The crater rim is to the left and the crater floor is to the right. The yellow arrows indicate a reversal of contrast between the direct and indirect illumination images. The blue arrows indicate where streaks transition to high-reflectance in the indirect illumination image (mean phase angles below $\sim 80^\circ$).

angle to all other pixels in the map) were calculated for each pixel within the crater using the SLDEM. The primary illumination was then paired with the viewfactor maps to produce an integrated map of indirect illumination inside the shadowed crater (each pixel receives secondary illumination from many other pixels).

The illumination models allow for the tracking of local illumination and viewing angles, which is essential because they vary considerably across the field of view and even within a single pixel. Under direct solar illumination, a single phase angle is assigned to each pixel and varies by only $\sim 5^\circ$ over the NAC field of view (~ 5 km). However, under indirect lighting, the phase angle can vary by $\sim 30^\circ$ within a single pixel (Fig. 2C) and the mean can vary by $\sim 20^\circ$ over the NAC field of view (Fig. 1D) [6,7].

Results: We have mapped features observed under direct and indirect illumination in ten representative craters; Lalande A is highlighted here as an example.

High reflectance mass-wasting streaks are commonly visible on crater walls in direct illumination images at low incidence and phase angles (Fig. 1A; expanded in 2A). However, under indirect illumination, the relative reflectance compared to the substrate varies (Fig. 1B; expanded in 2B). Near the floor of the crater, the streaks exhibit relatively high reflectance, while in other areas close to the rim, there is a contrast reversal (low-reflectance streak) or no reflectance signature along the same streak. This variable contrast is likely due to a combination of factors. Near the crater rim (left side of Fig. 2) the mean phase angle is near 90° , and only exposures of very high albedo material remain high in reflectance. Notably, this region appears to be a blocky outcrop of immature material based on SLDEM slope map and meter-scale NAC images, rather than a granular flow. Where material flowed downslope, the surface texture

appears to have a large effect on reflectance, and the small-scale shadows of a rougher surface may overcome the albedo, resulting in a streak with reflectance that is either lower than or comparable to its surroundings. Near the crater floor (right side of Fig. 2) the mean phase angles drop below 80° and the high-albedo material (direct illumination image) is discernable in the indirect lighting images as the shadowing effect caused by the increase in surface roughness is reduced.

Reflectance variations between direct and indirect illumination images are similar for craters with high-reflectance ejecta (HRE). For example, 33 HRE craters are visible within Lalande A, only 3 are observed in the indirect illumination images, and all are found where mean phase angles are $< 80^\circ$ (Fig. 1), which is similar to direct lighting images where albedo signatures are suppressed at higher phase angles.

Roughness and albedo are well known to have large effects on reflectance that vary with phase angle [8]. Our initial observations suggest that the highly variable phase angles within a scene add an additional complication to interpreting scenes with indirect illumination: some regions have phase angles low enough such that albedo variations can be observed, whereas in other portions of the same image, surface textural differences have the larger effect on reflectance. This high degree of local variation in phase angle and resulting visibility of albedo differences highlights the importance of modeling the complex phase angles observed in PSRs, where no images with direct illumination are available for comparison.

References: [1] Speyerer et al., 2013, *Icarus*, 222, 122-136. [2] Robinson et al., 2010, *Sp. Sci. Rev.*, 150, 81-124. [3] Robinson, M. S., 2018, *LPV*, Abstract #5028. [4] Raney et al., 2011, *Proc. IEEE*, 99, 808-823. [5] Barker et al., 2016, *Icarus*, 273, 346-355. [6] Thompson et al., 2018, *Informatics and Data Analytics*, Abstract #6037. [7] Thompson et al., 2019, *LPSC*, Abstract #3100. [8] Hapke, B., 1981, *JGR*, 86, 3039-3054.